Jurnal Teknologi
https://jitekin-upiyptk.org/ojs
2023 Vol. 13 No. 2 Hal: 58-64 p-ISSN: 2301-4474, e-ISSN: 2541-1535

Bead Characterization for Wire Based Laser Directed Energy Deposition Fabrication Process

Muhammad Irfan Syahmi Sidun[1], Ismayuzri Ishak[2]✉

[1,2]Faculty of Manufacturing and Mechatronic Engineering Technology, Universiti Malaysia Pahang Al-Sultan Abdullah, 26600 Pahang, Malaysia.

yuzriishak@ump.edu.my

Abstract

A three-dimensional, solid object of almost any shape or design can be created using metal additive manufacturing, often known as metal 3D printing. One of the most popular materials utilized in additive manufacturing is metal. The far more complicated procedure of directed energy deposition (DED) is frequently employed to upgrade or repair existing components. DED fabrication process will be able to construct a 3D metal object with consideration of the weld bead characteristics. Without knowing the weld bead characteristics, the mechanical integrity will not hold as the bead size is not suitable for the product. In the current study, we will study the effect of variation of parameters of the DED machine to be able to print in a continuous deposition and we will also investigate the weld bead characteristics printed by the variation of parameters with the use of DED machine. The variation of parameters of the machine are the laser power with the unit of Watt and the feedrate of the machine with the unit of mm per minute. Nine preliminary samples are printed to check whether the bead can be printed in a continuous line or not. The value of variation of parameters that bring about a continuous deposition will be jotted and continued to be taken to bead characterization for study. Six samples were printed, and the bead width and height are calculated based on the variation of parameters. Based on the result, we found that laser power will increase the bead width, but the bead height needs optimal laser power which is at 473 Watt and optimal feedrate which is on 60 mm per min to reach optimal bead height which is at 2.1162 mm. The effect of the machine feedrate on the other hand is inconsistent, thus more samples need to be gathered.

Keywords: Bead Characterization, Directed Energy Deposition, Wire Directed Energy Deposition, Mild Steel

1. Introduction

Additive Layer Manufacturing (ALM) or Additive Manufacturing (AM) is generally the ability to procure materials using a variety of techniques to produce 3D objects [1], [2]. The computer-aided design (CAD) software or 3D scanner-created threedimensional (3D) model is used as the source of data and information for the additive manufacturing process. To build an object with precise geometric shapes and designs, one can currently use a variety of additive manufacturing procedures or techniques [3], [4]. One of the most common ALM processes used nowadays is Directed Energy Deposition (DED) fabrication process (Figure 1) [5], [6]. In the DED process, the materials are fused while being deposited one layer at a time on a substrate using thermal energy (such as a laser, electron beam, or kinetic energy). The raw materials are fed into the build chamber by blowing powder via several nozzles, in wire form, as mixes of gases, or both. It is a fusion-based process that uses a lot of energy [7], [8]. For functionally graded pieces, multiple materials may be placed simultaneously. Despite having distinct characteristics, DED processes have only had a modest amount of success in the ALM industry. For instance, many materials can be deposited at once, enabling the creation of functionally graded pieces [9]. [10]. The DED process can be used to add material to an existing part to repair damaged or worn-out tools or parts [11]. [12].

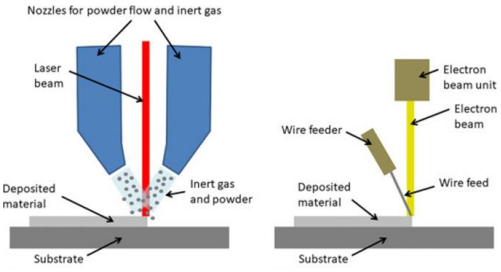

(a) (b)

Figure 1: Diagrams of two DED systems: (a) employs a laser and powder feedstock, whereas (b) uses an electron beam and wire feedstock

Most suitable and economically DED processes are Wire-DED. Metallic wire is used as the feed stock and an electric arc, laser, or electron beam is used as the energy source in the wire-DED additive layer manufacturing (ALM) process. Arc DED, laser-wire DED, and electron-beam DED are all distinctive AM

Accepted: 20-11-2023 | Revision: 24-12-2023 | Publication: 31-12-2023 | doi: 10.35134/jitekin.v13i1.98

processes that each type of heat source produces. But they all have one thing in common: the energy source melts a wire of metal that is continuously supplied into the process, depositing the molten metal along a predefined path. Simpleness, flexibility, high deposition rates, and the capacity to create large-scale parts with great structural integrity are all benefits of wire DED [13], [14]. W-DED AM processes are capable of producing large-scale and nearly-net-shape metallic components in a variety of industrial sectors, including aerospace, aviation, and power generation, compared to powder-based approaches, they have much higher deposition rates and less material waste [15], [16].

In summary, Wire-Directed Energy Deposition (Wire-DED) fabrication process is a fantastic technological innovation with a faster build rate compared to other metal additive manufacturing processes due to its high deposition rate at a relatively low resolution. However, beads procured by Wire-DED will greatly vary depending on the parameters of the printing machine. Considering this, this study will examine each bead procured by Wire-DED fabrication process by influencing the parameters of the printing machine and investigate the mechanical properties of 3D objects procured by the selection of beads.

2. Related Work

In general, additive manufacturing has provided us with many methods for the creation of objects using metal. Directed energy deposition works by melting the metal wire by using laser to create what we call beads. Bead sizes differ and are affected by many factors. Only by altering variables like laser power, feed rate, wire feed, etc. can the shape of the beads be optimized [17]. [18] examined how the process and bead characteristics were affected by the wire formation, wire feed, laser bit range, and laser power. They discovered that it is crucial to maintain a laser bit range that is as huge as the anticipated melt pool and, consequently, as huge as the bead size. [19] additionally established process diagram that was created to anticipate the process parameters and bead shape for the fiber laser deposition of Inconel 625 wire. They stated that both the deposition process parameters and the geometrical properties of beads are significantly influenced by energy per unit length and wire deposition volume per unit length. A stationary laser beam in the shape of a bar to study the form of the deposition's beads was used [20]. By altering the energy of the laser and wire feed rate of the wire in the appropriate ranges, the layer height and layer width could be controlled effectively. The range of bead shapes was constrained, nevertheless, because of the shape restriction on the laser beam.

3. Research Method

3.1. Wire-Directed Energy Deposition (W-DED)

Since the wire-DED process relies on melting and solidification, the fundamental understanding and expertise gained through welding metallurgical mechanism can be helpful. The components produced by wire-DED have a microstructure that is distinctly different from those of processes thanks to this complex thermal behavior. For this research, the architecture of the system will be explored to fully grasp the fundamentals behind the W-DED fabrication process.

Panasonic MCDHT3520E acts as the controllers for x, y and z axis. The AC Servo Motor & Driver, MINAS A5-series is a well-known servo system that satisfies all requirements from a range of machines, whether they need high speed, high precision, and high performance or just simple settings. Products from the A5-series offer better performance than those from the previous A4-series while only requiring little setup and user customization. The output range of newly developed motors, which have a 20-bit incremental encoder and less cogging torque, ranges from 50 W to 15.0 kW. These motors guarantee greater stability when used with low-stiffness machinery and fast, precise operation when used with stiffness machinery. They can be utilized in a number of different machine combinations.

BCL4516E is an I/O extension module designed to give the FSCUT control system greater I/O resources. Additionally, the BCL4516E offers two channels of DA output and one additional servo control connector. applied in applications that require additional I/O resources, such as pallet changers and auto loading. Sensors DA and AD with 12-bit with an accuracy of ±10mV. PWM 1 5V/24V for options with an accuracy for 5kHz ±0.3% and the highest is 50kHz. 1% common output pulse 16 relay output that provide normal-open and normal-close contact 1 PUL+/-, DIR+/- differential output, highest output frequency direction Encoder 1 A+/A-, B+/B-, Z+/Z-. The highest input frequency is 223kHz 2 positive, negative signal. Dedicated limit input low-level active 1 origin input (<15.8V) input.

The majority of 3D printers are controlled by RAMPS, or RepRap Arduino Mega Pololu Shield. It is made to fit all of the electronics required for a RepRap into a small, inexpensive package. RAMPS provides plenty of potential for growth and connects an Arduino Mega to the robust Arduino MEGA platform. On a single Arduino MEGA shield, the modular design comprises plug-in stepper drivers and extruder control circuits. It makes use of Pololu Stepper Drivers that can step up to 1/16 of a step. The majority of 3D printers require four drivers, with three running to the axis and one driving

the extruder. For extra uses, a fifth stepper driver socket is an optional feature. The board features three high-power MOSFETS outputs that are fused to 5 A and 11 A printbed and extruder outputs. The following characteristics of the RAMPS board electronics package are RAMPS 1.4 (Figure 2) contains up to 5 outputs for stepper motor drivers. Secondly, there are 3 MOSFET powered outputs under PWM control. Next, the control pins for the heated bed and the extruder with an 11A fuse. 6 sets of digital pins with VCC and GND for endstops are in headers. Lastly, PWM, digital, serial, SPI, I2C, and analogue pins were added.

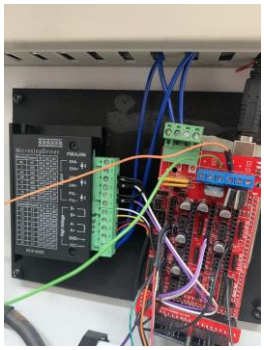

Figure 2. RAMPS board using RAMPS 1.4, contains up to 5 outputs for stepper motor drivers.

The laser that is used as the component to create the weld bead is IPG Laser. The model for the IPG Laser is YLS-2000-CUT SERIES-QCW Quasi-CW with Ytterbium Laser System. 20 kW of high peak power, pulse lengths of 0.2 to10 ms, and 200 J pulse power maximum are all delivered by the YLS-2000-CUT SERIES-QCW Quasi-CW fiber laser at repetition rates up to 2 kHz.

Table 1. Optical characteristics of Ytterbium Laser System

Characteristics	Test conditions	Symbol	Min.	Typ.	Max.	Unit
Operation Mode			CW/Modulated			
Polarization			Random			
Nominal Output Power		P_{nom}	2000			W
Output Power Tuning Range		λ	10		105	%
Emission Wavelength	Output power: 2000 W	$\Delta\lambda$	1068		1080	nm
Emission Linewidth	Output power: 2000 W			3	6	nm
Switching ON/OFF Time	Output power: 2000 W			50	100	μs
Output Power Modulation Rate	Output power: 2000 W				5	kHz
Output Power Instability	Output power: 2000 W			± 1	± 2	%
Red Guide Laser Power	Output power: 2000 W		0.4	0.5		mW

3.2. ER70S-6 Mild Steel Wire

The American Welding Society (AWS) classifies ER70S-6 as a common welding wire for carbon steel solid wire electrodes. It is primarily intended for Metal Inert Gas (MIG) or Gas Metal Arc (GMAW) welding procedures. The ER70S-6 is well renowned for its adaptability and is frequently used in a variety of sectors, including manufacturing, construction, and the automobile industry. The label "ER" stands for "Electrode Rod," indicating that it is a wire electrode that may be used again. The number "70" denotes the lowest achievable tensile strength in ksi (kips per square inch) for the welding metal following welding. To improve the weld quality and prevent porosity, deoxidizers and other components have been added to the wire's composition, as indicated by the "S" symbol. The number "6" denotes the wire's degree of cleanliness and weldability. Carbon steel makes up ER70S-6, which also frequently has trace levels of silicon and manganese that aid in deoxidizing the weld and improving arc stability. Additionally, these components provide enhanced penetration, wetting action, and overall weld quality. A copper layer is applied to the wire to improve electrical conductivity and prevent corrosion. This material is suitable for Directed Energy Deposition (DED) fabrication process.

Table 2. The elemental composition of ER70S-6

Element	C	Ni	Cr	Mo	Mn	Si	Cu	P	V	S
%	0.06-0.15	0.15	1.15	0.15	1.4-1.85	0.80-1.15	0.50	0.025	0.03	0.035

3.3. Characterization Method

To characterize, we got to calculate the weld bead characteristics fabricated by using the W-DED machine. There are three determining factors to define weld bead characteristics which are the width of bead (Figure 3), the height of the bead, and the deposited area.

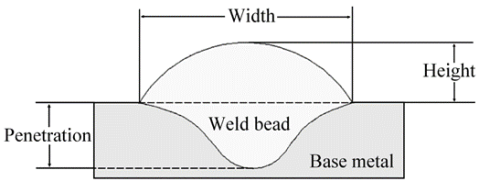

Figure 3. Weld Bead Characteristics

To calculate the weld bead characteristics, we will calculate the width and height manually by utilizing the multitude of measurement tools at our disposal.

3.4. Optical Video Measurement System

Since the bead size would be quite small, special tools must be utilized to calculate welding bead characteristics. This is where optical video measurement systems come in hand. This tool would be able to observe the bead characteristics even in miniscule size. This product in particular utilized the software Precision Plotter MV8 V7.1.34 to calculate the distance between the points of interest. The distance would then be presented in mm as the software would be able to calculate the focal length and the projected image length and then would be converted to real time distance (Figure 4).

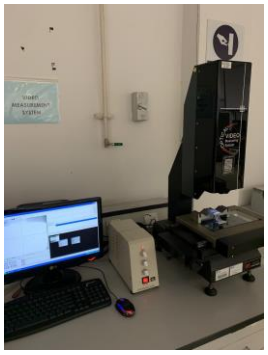

Figure 4. Optical Video Measuring System

4. Results and Discussions

4.1. Preliminary Results

Preliminary results are important as to determine the scope of our research. 9 samples have been collected to pick a range of samples to be investigated. In Table 9, all samples are shown with a variation of parameters that greatly affect the continuous deposition of bead. Figure 5 are shown as an example of a non-continuous bead deposition meanwhile Figure 6 are shown as an example of a continuous bead deposition. Hence, we choose a range of samples from sample 3 to sample 8. These samples will then be printed on a rectangular mild steel plate.

Table 3. Preliminary sample table

Sample	Laser Power (W)	Feedrate (mm/min)	Continuous Deposition
Sample 1	393	40	N
Sample 2	393	45	No
Sample 3	393	50	Yes
Sample 4	393	55	Yes
Sample 5	393	60	Yes
Sample 6	473	60	Yes
Sample 7	473	65	Yes
Sample 8	473	70	Yes
Sample 9	473	75	No

Figure 5. A non-continuous bead deposition

Figure 6. A continuous bead deposition

4.2. Experimental Results

Six samples were produced by W-DED machine with each sample a different value of parameters of the machine. The width of substrate plate is important as the substrate plate width decreases, the easier it is to bend because of the heat of the laser. The width of the substrate plate is determined to be 3 mm as the plate will only need to handle a continuous deposition in 50 mm without bending while in fabrication process. After the bead has been procured on the mild steel substrate plate, a cross section cut of the sample would be the next step. The cross-section cut is important to observe the width and height of the bead with much detail. Figure 7 shows the collaged view of cross section cut of the width and height of the bead using Optical Video Measuring System. Table 4 shows the value of the output obtained based on Figure 7.

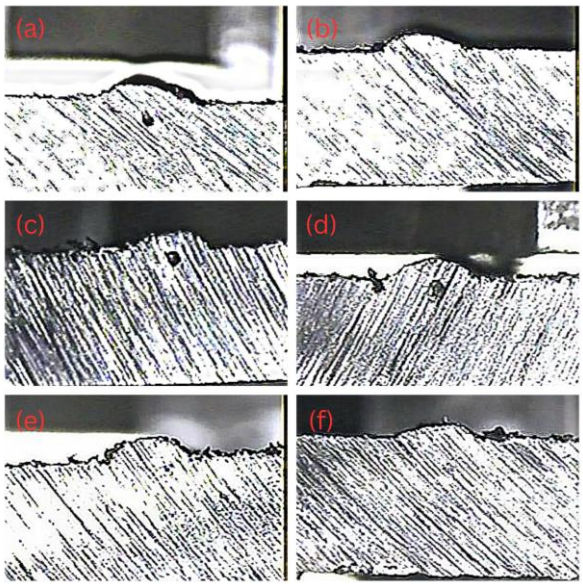

Figure 7. Collaged views of bead samples using Optical Video Measuring System ((a) Sample 1, (b) Sample 2, (c) Sample 3, (d) Sample 4, (e) Sample 5, (f) Sample 6).

The sample table (Table 4) has been created, a graph must be established to see the relationship between the variation of parameters and the weld bead characteristics. The welding bead characteristics are the welding bead width and the welding bead height.

The graph (Figure 1) had been established for the relationship between laser power and bead width. For the first set, the value 1.7634 mm increases to 2.1162 mm with the laser power increases from 393 Watt to 473 Watt. For the second set, the value of bead width 1.7013 mm increases to 1.8712 mm. For the last set, the bead width value decreases slightly from 1.8672 mm to 1.888 mm.

Table 4. Sample table

Sample	Laser Power (W)	Feedrate (mm/min)	Bead height (mm) ±0.0001	Bead width (mm) ±0.0001
Sample 1	393	50	1.7634	0.4530
Sample 2	393	55	1.7013	0.4119
Sample 3	393	60	1.8672	0.4530
Sample 4	473	60	2.1162	0.5354
Sample 5	473	65	1.8712	0.5152
Sample 6	473	70	1.8880	0.3089

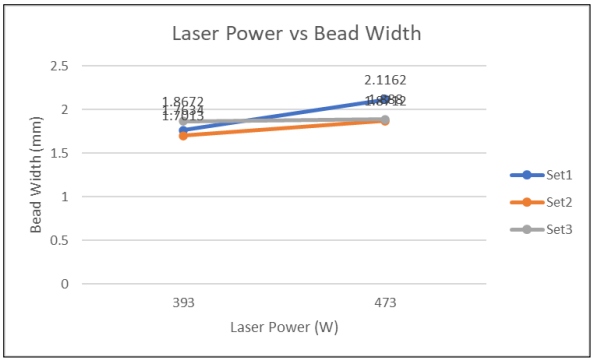

Figure 1. Relationship between laser power and bead width

The graph (Figure 2) had been established for the relationship between laser power and bead height. For the first set, the value 0.453 mm increases to 0.5354 mm with the laser power increases from 393 Watt to 473 Watt. For the second set, the value of bead width 0.4119 mm increases to 0.5152 mm. For the last set, the bead width value decreases slightly from 0.453 mm to 0.3089 mm.

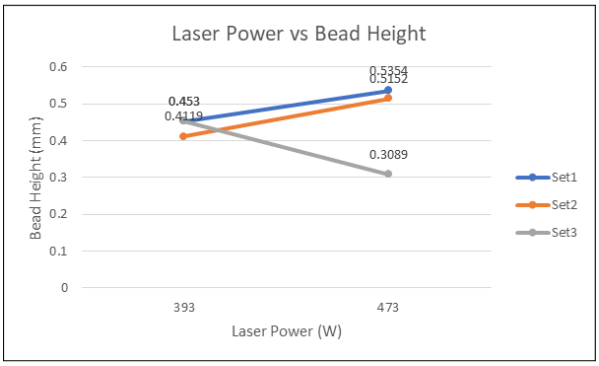

Figure 2. Relationship between laser power and bead height

The graph (Figure 3) had been established for the relationship between machine feed rate and bead width with the laser power at a constant 473 Watt. Starting from 60 mm per min, the bead width at 2.1162 mm decreases to 1.8712 mm at 65 mm per min and increases back to 1.888 mm at 70 mm per min.

While, the graph (Figure 4) had been established for the relationship between machine feedrate and bead width with the laser power at a constant 473 Watt. Starting from 60 mm per min, the bead width at 2.1162 mm decreases to 1.8712 mm at 65 mm per min and increases back to 1.888 mm at 70 mm per min.

The graph (Figure 5) has been established for the relationship between machine feedrate and bead height with the laser power at a constant 393 Watt. Starting from 50 mm per min, the bead height at 0.453 mm decreases to 0.4119 mm at 55 mm per min and increases back to 0.453 mm at 60 mm per min.

Moreover, the graph (Figure 6) had been established for the relationship between machine feedrate and bead height with the laser power at a constant 473 Watt. Starting from 60 mm per min, the bead height at 0.5354 mm decreases to 0.5152 mm at 65 mm per min and keeps decreasing to 0.3089 mm at 70 mm per min.

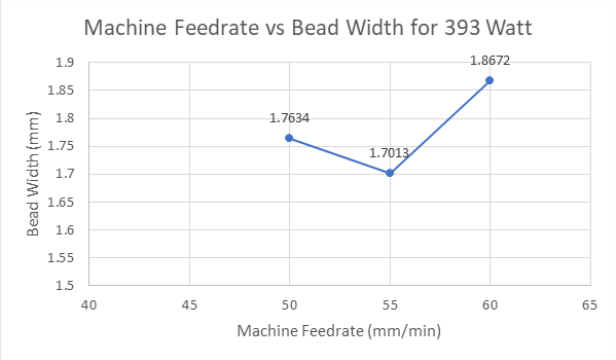

Figure 3. Relationship between machine feedrate and bead width with the laser power at a constant 393 Watt.

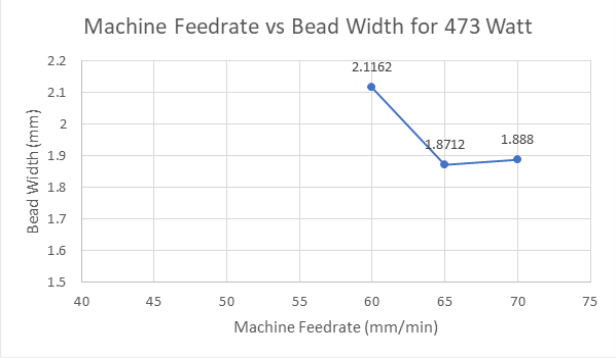

Figure 4. Relationship between machine feedrate and bead width with the laser power at a constant 473 Watt.

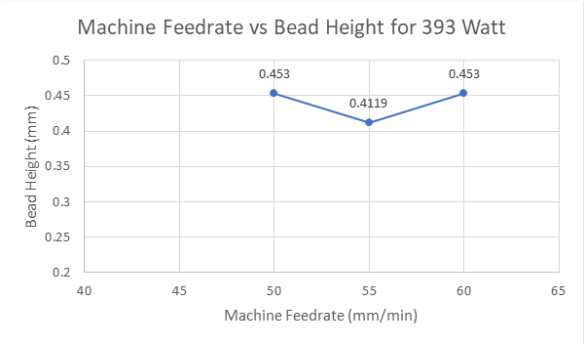

Figure 4. Relationship between machine feedrate and bead height with the laser power at a constant 393 Watt.

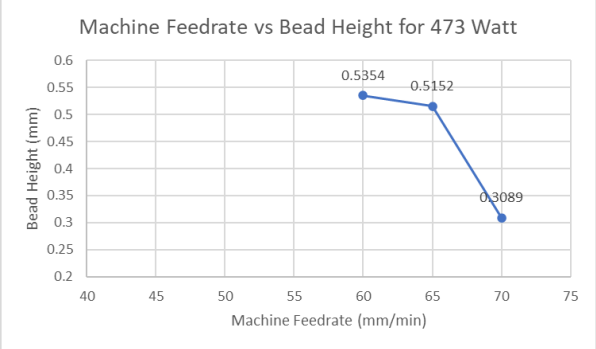

Figure 5. Relationship between machine feedrate and bead width with the laser power at a constant 473 Watt.

5. Conclusion

This study focused on analyzing the weld bead procured by directed energy deposition fabrication process by measuring the weld bead characteristics. The main concept of this study was to study the correlation between variation of parameters and the weld bead characteristics procured in a continuous line by directed energy deposition fabrication process. Based on the experimental results, a few conclusions and recommendations have been made. First, we know that laser power directly controls the weld bead characteristics, as the laser power increases the bead width also increases as it is the effect of melt pool. Next, we also know that the optimal bead height would need specific values of the parameters of the machine. Based on our results, the laser power would be at 473 Watt and the feed rate would be at 60 mm per min. Lastly, we know that the effect of machine feed rate on bead width and bead height on the other hand is inconsistent as the value fluctuates with instability. To find the optimal value for both weld bead characteristics, the machine feed rate would increment the value of 5 mm per min and more samples must be gathered.

Acknowledgements

The authors would like to thank the management and staff of the Faculty of Manufacturing and Mechatronic Engineering Technology, Universiti Malaysia Pahang Al-Sultan Abdullah, for their relentless support.

References

[1] Chandima Ratnayake, R. M. (2019). Enabling RDM in challenging environments via additive layer manufacturing: enhancing offshore petroleum asset operations. Production Planning & Control, 30(7), 522-539. https://doi.org/10.1080/09537287.2018.1540054

[2] Hajare, D. M., & Gajbhiye, T. S. (2022). Additive manufacturing (3D printing): Recent progress on advancement of materials and challenges. Materials Today: Proceedings, 58, 736-743. https://doi.org/10.1016/j.matpr.2022.02.391

[3] Vaneker, T., Bernard, A., Moroni, G., Gibson, I., & Zhang, Y. (2020). Design for additive manufacturing: Framework and methodology. CIRP Annals, 69(2), 578-599. https://doi.org/10.1016/j.cirp.2020.05.006

[4] Careri, F., Khan, R. H., Todd, C., & Attallah, M. M. (2023). Additive manufacturing of heat exchangers in aerospace applications: a review. Applied Thermal Engineering, 121387. https://doi.org/10.1016/j.applthermaleng.2023.121387

[5] Saboori, A., Gallo, D., Biamino, S., Fino, P., & Lombardi, M. (2017). An overview of additive manufacturing of titanium components by directed energy deposition: microstructure and mechanical properties. Applied Sciences, 7(9), 883. https://doi.org/10.3390/app7090883

[6] Saboori, A., Aversa, A., Marchese, G., Biamino, S., Lombardi, M., & Fino, P. (2019). Application of directed energy deposition-based additive manufacturing in repair. Applied Sciences, 9(16), 3316. https://doi.org/10.3390/app9163316

[7] Özel, T., Shokri, H., & Loizeau, R. (2023). A review on wire-fed directed energy deposition based metal additive manufacturing. Journal of Manufacturing and Materials Processing, 7(1), 45. https://doi.org/10.3390/jmmp7010045

[8] E. Pei, I. R. Kabir, D. Godec, J. Gonzalez-Gutierrez, and A. Nordin, Functionally graded additive manufacturing. INC, 2021. https://doi.org/10.1016/B978-0-12-823152-4.00006-5

[9] Feenstra, D. R., Banerjee, R., Fraser, H. L., Huang, A., Molotnikov, A., & Birbilis, N. (2021). Critical review of the state of the art in multi-material fabrication via directed energy deposition. Current Opinion in Solid State and Materials Science, 25(4), 100924. https://doi.org/10.1016/j.cossms.2021.100924

[10] Singh, D. D., Arjula, S., & Reddy, A. R. (2021). Functionally graded materials manufactured by direct energy deposition: a review. Materials Today: Proceedings, 47, 2450-2456. https://doi.org/10.1016/j.matpr.2021.04.536

[11] Marya, M., Singh, V., Hascoet, J. Y., & Marya, S. (2018). A metallurgical investigation of the direct energy deposition surface repair of ferrous alloys. Journal of Materials Engineering and Performance, 27, 813-824. https://doi.org/10.1007/s11665-017-3117-5

[12] Pathania, A., Kumar, S. A., Nagesha, B. K., Barad, S., & Suresh, T. N. (2021). Reclamation of titanium alloy based aerospace parts using laser based metal deposition methodology. Materials Today: Proceedings, 45, 4886-4892. https://doi.org/10.1016/j.matpr.2021.01.354

[13] Piscopo, G., & Iuliano, L. (2022). Current research and industrial application of laser powder directed energy deposition. The International Journal of Advanced Manufacturing Technology, 119(11-12), 6893-6917. https://doi.org/10.1007/s00170-021-08596-w

[14] Özel, T., Shokri, H., & Loizeau, R. (2023). A review on wire-fed directed energy deposition based metal additive manufacturing. Journal of Manufacturing and Materials Processing, 7(1), 45. https://doi.org/10.3390/jmmp7010045

[15] Altıparmak, S. C., & Xiao, B. (2021). A market assessment of additive manufacturing potential for the aerospace industry. Journal of Manufacturing Processes, 68, 728-738. https://doi.org/10.1016/j.jmapro.2021.05.072

[16] Wu, Y., Fang, J., Wu, C., Li, C., Sun, G., & Li, Q. (2023). Additively manufactured materials and structures: A state-of-the-art review on their mechanical characteristics and energy absorption. International Journal of Mechanical Sciences, 108102. https://doi.org/10.1016/j.ijmecsci.2023.108102

[17] Chen, G., Williams, S., Ding, J., Wang, C., & Suder, W. (2022). Multi-energy source (MES) configuration for bead shape control in wire-based directed energy deposition (w-DED). Journal of Materials Processing Technology, 304, 117549.https://doi.org/10.1016/j.jmatprotec.2022.117549

[18] Schulz, M., Klocke, F., Riepe, J., Klingbeil, N., & Arntz, K. (2019). Process optimization of wire-based laser metal deposition of titanium. Journal of Engineering for Gas Turbines and Power, 141(5), 052102.https://doi.org/10.1115/1.4041167

[19] Abioye, T. E., Folkes, J., & Clare, A. T. (2013). A parametric study of Inconel 625 wire laser deposition. Journal of Materials Processing Technology, 213(12), 2145-2151. https://doi.org/10.1016/j.jmatprotec.2013.06.007

[20] Mok, S. H., Bi, G., Folkes, J., & Pashby, I. (2008). Deposition of Ti–6Al–4V using a high power diode laser and wire, Part I: Investigation on the process characteristics. Surface and Coatings Technology, 202(16), 3933-3939. https://doi.org/10.1016/j.surfcoat.2008.02.008